Collisionally Regenerated Dark Matter Structures in Galactic Nuclei

David Merritt
Rochester Institute of Technology

Stefan Harfst
Rochester Institute of Technology

Bertone Gianfranco
INFN Sezione di Padova

Collisionally Regenerated Dark Matter Structures in Galactic Nuclei

David Merritt[*] and Stefan Harfst[†]

Department of Physics, Rochester Institute of Technology,
85 Lomb Memorial Drive, Rochester, NY 14623

Gianfranco Bertone[‡]

INFN, Sezione di Padova, Via Marzolo 8, Padova, I-35131, Italy
(Dated: February 5, 2008)

We show that the presence of a $\rho \sim r^{-3/2}$ dark matter overdensity can be robustly predicted at the center of any galaxy old enough to have grown a power-law density cusp in the *stars* via the Bahcall-Wolf mechanism. Using both Fokker-Planck and direct N-body integrations, we demonstrate collisional generation of these dark matter "crests" (Collisionally REgenerated STructures) even in the extreme case that the density of both stars and dark matter were previously lowered by slingshot ejection from a binary supermassive black hole. The time scale for collisional growth of the crest is approximately the two-body relaxation time as defined by the stars, which is $\lesssim 10$ Gyr at the centers of stellar spheroids with luminosities $L \lesssim 10^{9.5} L_{\odot}$, including the bulge of the Milky Way. The presence of crests can robustly be predicted in such galaxies, unlike the steeper enhancements, called "spikes", produced by the adiabatic growth of black holes. We discuss special cases where the prospects for detecting dark matter annihilations from the centers of galaxy haloes are significantly affected by the formation of crests.

PACS numbers: Valid PACS appear here

I. INTRODUCTION

While the evidence for a dynamically significant component of dark matter (DM) on cosmological scales is compelling, the nature of the DM is unknown, and its distribution on sub-galactic scales remains uncertain. A widely discussed DM candidate is the supersymmetric neutralino [1, 2], the presence of which might be detected indirectly through the products (gamma rays, neutrinos, anti-matter) of its self-annihilations [3, 4]. In the case of photons, the annihilation signal is simply proportional to the square of the DM density ρ_{χ} integrated along the line of sight, and most discussions of indirect detection have focussed on the centers of galaxies, including the Milky Way galaxy, where the DM density is likely to be highest [5, 6, 7, 8, 9].

Supermassive black holes (SBHs) are believed to be generic components of galactic nuclei [10] and are expected to strongly influence the distribution of mass (stars, DM) at distances $\lesssim r_h$ from the SBH [11], where r_h is the gravitational influence radius, defined as the radius within which the gravitational force from the SBH dominates that from the stars. In the case of the Milky Way SBH, $r_h \approx 3$ pc. In one widely discussed model [12], a so-called *spike* forms around the SBH at $r \lesssim r_h$ as it grows adiabatically. The density in such a spike is a steep function of radius near the SBH, $\rho_{\chi} \sim r^{-\gamma}$, $\gamma \gtrsim 2$ implying a large DM annihilation rate [12, 13, 14]. However the formation of such spikes requires finely-tuned initial con-

ditions [15] and the spikes are easily destroyed [16, 17]. Furthermore, the stars would react in the same was as the DM to spherically-symmetric growth of a SBH [11], and in the galaxies with long central relaxation times where steep stellar cusps could persist for 10 Gyr or longer, none are seen [11]. In such galaxies, stellar density profiles are typically flat at $r \lesssim r_h$, believed to be a consequence of the "scouring" effect of binary SBHs during galaxy mergers [18]. The density of DM at the centers of these galaxies would also presumably be low.

Steeply-rising stellar densities *are* instead observed at $r \lesssim r_h$ in the bulge of the Milky Way and possibly in M32, a nearby dwarf elliptical galaxy [19, 20]. In both of these dense, compact stellar systems, the two-body relaxation time near the SBH – the time for stars to exchange orbital energy via gravitational encounters – is $\lesssim 10^{10}$ yr, short enough for the formation of a Bahcall-Wolf [21] ("collisional") density cusp in the stars around the SBH, $\rho_{\star} \sim r^{-7/4}$. In dense galaxies like these, a Bahcall-Wolf cusp in the stars can even re-form after being destroyed by a binary SBH [22].

In this paper, we discuss the evolution of the DM density in a nucleus that grows a collisional cusp in the stars via the Bahcall-Wolf mechanism. The DM particles are essentially collisionless, but they scatter off of stars [23, 24, 25], forming a $\rho_{\chi} \sim r^{-3/2}$ density "crest" (Collisionally REgenerated STructure) near the SBH in roughly one stellar relaxation time. Remarkably, as we show, this is true even in the case that the galaxy core was previously "scoured" by a binary SBH: DM particles are scattered by stars into regions of phase space corresponding to tightly-bound orbits around the SBH that were previously depleted by the binary.

In Sects. II and III we present Fokker-Planck, as well

[*]Electronic address: merritt@astro.rit.edu
[†]Electronic address: harfst@astro.rit.edu
[‡]Electronic address: bertone@pd.infn.it

as direct N-body, integrations of a combined, star+DM system around a central point mass that demonstrate the formation of crests on roughly a star-star relaxation time scale. Sect. IV discusses the envirnomental conditions necessary for the formation of crests; we show that these conditions are likely to be satisfied in stellar spheroids comparable in luminosity to that of the Milky Way or fainter, allowing us to robustly predict the presence of DM crests in these systems. In Sect. V we discuss special cases where the prospects for detecting dark matter annihilations from the centers of galaxy haloes are significantly affected by the formation of crests. Our conclusions are summarized in Sect. VI.

II. FOKKER-PLANCK TREATMENT

An approximate description of the combined evolution of stars and DM at the center of a galaxy is provided by the isotropic, multi-mass Fokker-Planck equation [26, 27, 28]. Let $f(E, m, t)dm$ be the number density in phase space of objects (stars, DM particles) in the mass range m to $m + dm$; $E \equiv -v^2/2 + \phi \geq 0$ is the binding energy per unit mass and $\Phi \equiv -\phi$ is the gravitational potential, assumed fixed in time. (In what follows, changes in f are only significant within the SBH's sphere of influence and the assumption of a fixed potential is reasonable.) Then

$$\frac{\partial f}{\partial t} = \frac{1}{4\pi^2 p} \frac{\partial}{\partial E} \left(m D_E f + D_{EE} \frac{\partial f}{\partial E} \right), \quad (1a)$$

$$D_E(E, t) = -16\pi^3 \Gamma \int_E^\infty dE' p(E') g(E', t), \quad (1b)$$

$$D_{EE}(E, t) = -16\pi^3 \Gamma \Big[q(E) \int_0^E dE' h(E', t) +$$
$$\int_E^\infty dE' q(E') h(E', t) \Big]. \quad (1c)$$

The function $p(E) = 4\sqrt{2} \int_0^{r_{max}(E)} dr r^2 \sqrt{\phi(r) - E} = -\partial q/\partial E$ is the phase space volume accessible per unit of energy, $\Gamma = 4\pi G^2 \ln \Lambda$, and $\ln \Lambda$ is the Coulomb logarithm. The functions g and h are moments over mass of f:

$$g(E, t) = \int_0^\infty f(E, m, t) m \, dm, \quad (2a)$$

$$h(E, t) = \int_0^\infty f(E, m, t) m^2 dm \quad (2b)$$

e.g. g is the phase-space mass density.

Consider now a nucleus containing just two components, stars of mass $m_\star$ and DM particles with an unspecified range of masses such that $m_\chi \ll m_\star$. Assume further that $g_\chi \ll g_\star$. Taking the first moment of Eq. (1a)

over mass then yields the two evolution equations

$$\frac{\partial g_\star}{\partial t} = \frac{1}{4\pi^2 p} \frac{\partial}{\partial E} \left(m_\star D_E g_\star + D_{EE} \frac{\partial g_\star}{\partial E} \right), \quad (3a)$$

$$\frac{\partial g_\chi}{\partial t} = \frac{1}{4\pi^2 p} \frac{\partial}{\partial E} \left(D_{EE} \frac{\partial g_\chi}{\partial E} \right), \quad (3b)$$

with diffusion coefficients

$$D_E(E, t) = -16\pi^3 \Gamma \int_E^\infty dE' p(E') g_\star(E', t), \quad (4a)$$

$$D_{EE}(E, t) = -16\pi^3 \Gamma m_\star \Big[q(E) \int_0^E dE' g_\star(E', t) +$$
$$\int_E^\infty dE' q(E') g_\star(E', t) \Big]. \quad (4b)$$

The DM particles, being of negligibly small mass, do not self-interact gravitationally and they evolve solely due to heating by (i.e. scattering off of) the stars [23, 24]. As a result, the characteristic time for change in either $g_\star$ or g_χ is the same, $(4\pi \Gamma m_\star g_\star)^{-1}$, equal to within a constant factor to the standard two-body relaxation time T_r defined by the stars alone [27]:

$$T_r \equiv \frac{0.065 v_{rms}^3}{G^2 m_\star \rho_\star \ln \Lambda}, \quad (5)$$

with v_{rms} the mean square velocity. In a time $\gtrsim T_r$, the stellar distribution approaches its steady-state form near the SBH,

$$g_\star(E) \sim E^{1/4}, \quad \rho_\star(r) \sim r^{-7/4}, \quad (6)$$

the so-called Bahcall-Wolf [21] solution. The steady-state solution for the DM is obtained by setting $\partial g_\chi / \partial E = 0$, or

$$g_\chi(E) \sim \text{const.}, \quad \rho_\chi(r) \sim r^{-3/2}, \quad (7)$$

[24, 25, 29]. Both of these solutions assume a non-evolving phase space density far from the SBH; in reality, the DM density will drop after the formation of the crest, due to ongoing heating by the stars [24], and under certain circumstances the stellar density may continue to evolve as well [11] (the functional form (7) of g_χ is unaffected by such evolution and we ignore it in what follows). While the solution (7) for g_χ at $r \ll r_h$ is independent of $g_\star$, the time required to attain this density profile, and the subsequent rate of heating by the stars, do depend on $g_\star$.

Fig. 1 shows time-dependent solutions to Eqs. (3a)-(4b). Initial density profiles for both the stars and DM were assigned as in Ref. [30]; these models have $\rho \propto r^{-\gamma}$ near the SBH, and we chose $\gamma = 0.5$, the flattest density profile consistent with an isotropic phase-space distribution in a $1/r$ potential. (The density at large radius in this model falls off more steeply than the $\rho_\chi \sim r^{-1}$ dependence predicted in standard DM halo models; however we are concerned here with the evolution only at very small
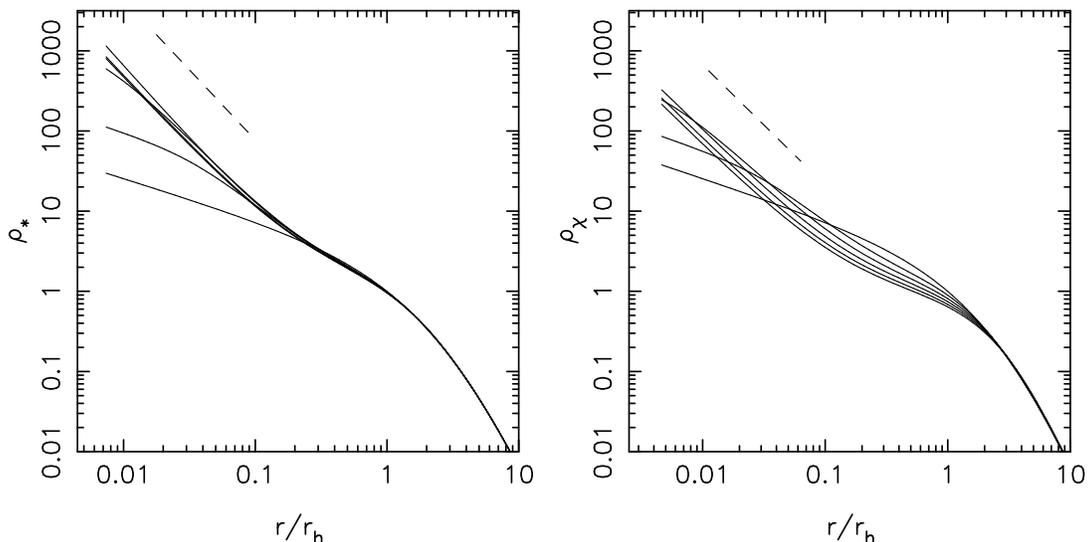
FIG. 1: Solutions of the Fokker-Planck equations (3a)-(4b) that describe the joint evolution of stars and dark matter around a black hole due to star-star and star-DM gravitational encounters. Length unit r_h is the radius containing a mass in stars equal to twice the black hole mass at $t = 0$ (roughly 3 pc at the Galactic center). Density is in units of its initial value at r_h. Curves show the stellar (left) and dark matter (right) density profiles at times $(0, 0.2, 0.4, 0.6, 0.8, 1.0)$ in units of the initial relaxation time (Eq. 5) at $r = r_h$. Dashed lines are the "steady-state" solutions, Eqs. (6) and (7).
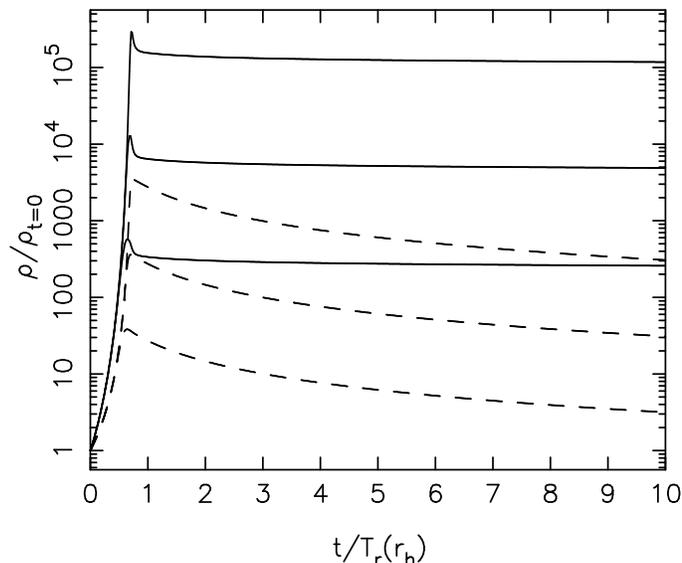

FIG. 2: Evolution of the stellar (solid lines) and dark matter (dashed line) densities at radii of $(10^{-5}, 10^{-4}, 10^{-3})r_h$ in the Fokker-Planck integration of Fig. 1. Densities are normalized to their values at $t = 0$.

radii.) The unit of time in Fig. 1 is the relaxation time for the stars at the influence radius r_h, defined in the standard way as the radius containing a mass in stars equal to twice $M_\bullet$. In principle, r_h so defined changes with time in response to the changing stellar density, but this effect is almost negligible and we ignore it in what follows.

In a time $\sim 0.5T_r(r_h)$, the stars are seen to attain the Bahcall-Wolf profile at $r \lesssim 0.2r_h$. The evolution of the DM is more complex. A $\rho_\chi \sim r^{-3/2}$ crest inside $r \approx 0.1r_h$ is formed in roughly the same time. However the amplitude of the crest drops thereafter as the DM is heated by the stars (Figs. 1,2): by a factor $1/e$ in a time of $\sim 1.2T_r(r_h)$ after peak density, and by a factor $1/e^2$ in a time of $\sim 4.5T_r(r_h)$. Evolution of the DM density profile after crest formation is approximately self-similar, $\rho_\chi(r,t) \approx \rho_{\chi,0}(r)G(t/T_r)$ at $r \lesssim r_h$, with $dG/dt < 0$.

III. N-BODY TREATMENT

The Fokker-Planck equations (3a)-(4b) embody a number of approximations (isotropy, small-angle scattering, uncorrelated encounters, fixed gravitational potential, etc.) that may be violated in real stellar systems. Furthermore the initial conditions of Fig. 1 are ad hoc. We therefore carried out a direct N-body integration of stars and massless particles around a point mass, starting from initial conditions that realistically represent the center of a galaxy after a binary SBH has created a low-density core [22].

The N-body code was adapted from φGRAPE [31], a direct-summation code that advances particles via a fourth-order integrator and computes gravitational forces via calls to special-purpose accelerator boards called GRAPEs [32]. The code was modified to run in serial mode using a single GRAPE-6 computer which has an onboard memory limit of $\sim 256K$ particles and a speed of ~ 1 Tflops. The code was also modified to include massless (DM) particles; since these do not "see" each other gravitationally, they need not all be loaded into GRAPE
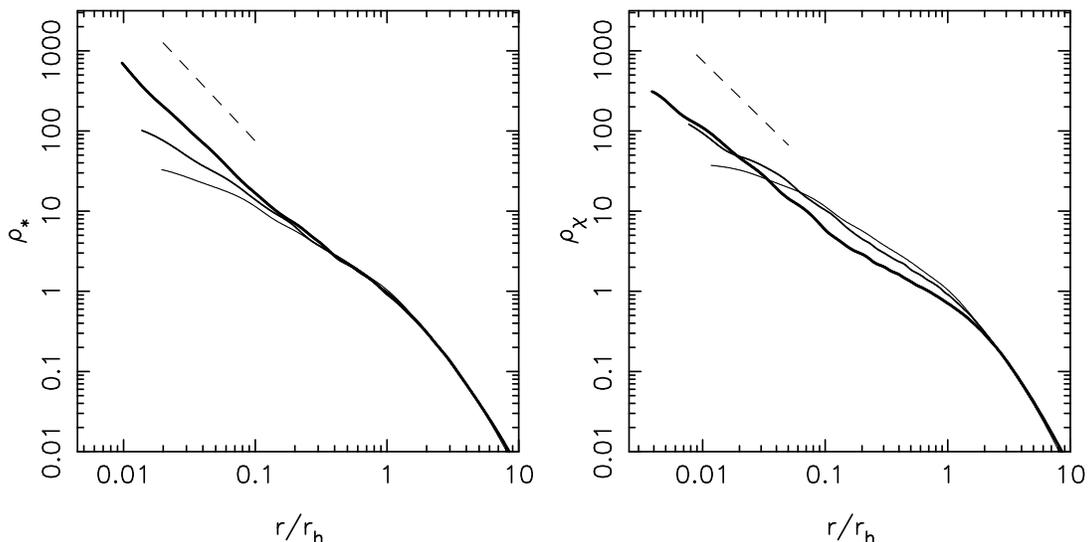
FIG. 3: Direct N-body integration of "star" (left) and "dark matter" (right) particles around a single massive particle ("black hole"), starting from a galaxy model in which a pre-existing binary black hole had created a low-density core [22]. Thin, normal and thick curves show the density profiles at times $(0, 0.25, 1.0)$ in units of $T_r(r_h)$. Dashed lines are as in Fig. 1.

memory simultaneously, allowing the GRAPE's memory limit to be circumvented. We used $N_\star = 1.2 \times 10^5$ "star" particles and $N_\chi = 2.4 \times 10^6$ "DM" particles.

Initial conditions for the N-body integration were adapted from Run 8 of Ref. [22]. In that paper, N-body simulations were used to follow the formation of low-density cores via inspiral of a SBH into the center of a galaxy containing a second, more massive SBH; in Run 8, the binary mass ratio was $1:4$. We replaced the two massive particles at the final time step of Run 8 by a single particle (the SBH) having their combined mass (0.0125 in units of the total galaxy mass), and positioned this particle at the center of mass of the pre-existing binary. Massless (DM) particles were then added via a bootstrap algorithm: a star particle was chosen at random; a DM particle was placed randomly on a sphere with radius equal to that of the star particle; the DM particle was assigned a velocity with random direction subject to the constraint that the radial and tangential components were equal to those of the star particle. This scheme produced a model in which the DM had the same initial phase-space distribution as the stars; in particular, both components had essentially flat central density profiles (Fig. 3). In addition, the velocity distributions at $r \lesssim r_h$ were biased toward circular motions, a result of gravitational slingshot ejection of particles on radial orbits by the binary. N-body integration of this model until a time $\sim T_r(r_h)$ using φGRAPE required ~ 43 d on the GRAPE-6 special-purpose computer, for a total of $\sim 6.6 \times 10^{17}$ floating-point operations.

Fig. 3 shows the results. The star particles form a Bahcall-Wolf cusp in a time $\sim 0.5 T_r(r_h)$. The response of the DM particles is also consistent with what was found in the Fokker-Planck integration (Fig. 1): formation of a crest at $r \lesssim 0.1 r_h$ and a gradual drop in ρ_χ as the DM

is heated by the stars. The DM density slope at $r \lesssim 0.01 r_h$ is not well constrained due to the finite number of particles but is consistent with $\rho_\chi \propto r^{-3/2}$. Henceforth we will assume that the Fokker-Planck solution correctly describes the radial dependence of the DM density at radii too small to be resolved via the N-body integration.

Both the size of the core formed by an inspiralling SBH (measured in units of the binary's mass) and the time scale to regrow a stellar cusp (measured in units of $T_r(r_h)$) are almost independent of the binary mass ratio [18, 22] and so the results of our single N-body integration should be representative of the majority of galactic nuclei that formed via mergers, if the length and mass are scaled to r_h and $M_\bullet$ respectively.

IV. GALAXY PROPERTIES RELEVANT TO THE FORMATION OF CRESTS

Several basic conditions must be satisfied for a DM crest to form in a galactic nucleus. (1) The two-body (star-star) relaxation time must be short. (2) The nucleus must contain a massive BH. (3) For the annihilation signal to be detectable, there must be a significant amount of DM on scales $\lesssim r_h$. In this section, we review current knowledge concerning physical conditions in galactic nuclei and discuss which kinds of galaxies are most likely to harbor DM crests.

A. Relaxation times

The two-component models presented above demonstrate that a stellar cusp and its associated DM crest are generated in a time of $\sim 0.5 T_r(r_h)$. (The single-
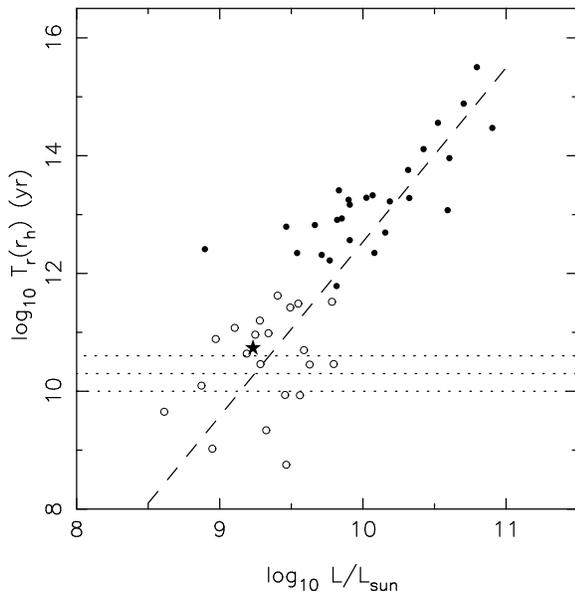
FIG. 4: Relaxation times at the SBH's influence radius r_h in Virgo cluster galaxies (circles) and the Milky Way (star) vs. the total blue luminosity of the galaxy (in the case of the Milky Way, the bulge). A stellar mass of $1M_\odot$ was assumed when computing T_r. Filled circles: Virgo cluster galaxies in which r_h is resolved, i.e. $r_h \geq 0.1''$. Open circles: Virgo cluster galaxies in which r_h is unresolved. Stellar luminosity profiles were taken from Ref. [33] and black hole masses were computed from the $M_\bullet - \sigma$ relation [10], except in the case of the Milky Way for which $M_\bullet$ has been directly determined from stellar orbits [34]. Horizontal dotted lines are at $T_r(r_h) = (1, 2, 4) \times 10^{10}$ yr. Dashed line is a regression fit to the data, Eq. 8.

component N-body studies in Refs. [22, 35, 36] reach similar conclusions about the time scale for stellar cusp formation.) Fig. 4 shows estimates of $T_r(r_h)$ vs. spheroid luminosity in a complete sample of early-type (elliptical and lenticular) galaxies in the Virgo cluster [33, 37] and the bulge of the Milky Way. (The spheroid is defined as the entire luminous galaxy in the case of elliptical and lenticular galaxies, and as the bulge component in the case of spiral galaxies.) There is a well-defined trend of $T_r(r_h)$ with spheroid luminosity L:

$$T_r(r_h) \approx 3.8 \times 10^9 \text{yr} \, L_9^{3.0} \quad (8)$$

where $L_9 \equiv L/10^9 L_\odot$. Spheroids with $L \lesssim 2 \times 10^9 L_\odot$ have $T_r(r_h) \lesssim 3 \times 10^{10}$ yr, which is short enough for the formation of a crest, assuming that the SBH and spheroid were in place at least $\sim 10^{10}$ yr ago. The Milky Way (marginally) satisfies this condition, and the Galactic center stellar cluster in fact has a density profile that is consistent the Bahcall-Wolf form [19, 20].

Conditions for the formation of crests are relaxed somewhat if there is a top-heavy spectrum of stellar masses since the DM scattering time scales as $\tilde{m}_\star^{-1}$ where $\tilde{m}_\star = \langle m_\star^2 \rangle / \langle m_\star \rangle$ [24]. The stellar cusp can also evolve more quickly in this case [38].

Unfortunately, in the luminosity range most relevant to DM crest formation, the Milky Way bulge is the *only* spheroid near enough for a Bahcall-Wolf cusp to be detected even if present. Spheroids fainter than $L \approx 10^9 L_\odot$ and outside the Local Group are always unresolved on scales $r \lesssim r_h$ (e.g. Fig. 4). However there are indications that nuclear structure begins to change systematically as L drops below $\sim 10^9 L_\odot$, since an increasingly large fraction of spheroids exhibit compact stellar nuclei [37, 39]. Only one compact nucleus is spatially well resolved, in the Local Group galaxy NGC 205 ($L \approx 10^{8.4} L_\odot$), and the relaxation time is found to drop to $\sim 10^8$ yr at the center [40]; this value is derived assuming no SBH since NGC 205 shows no evidence of rising velocities near the center [40]. Whether the compact nuclei in faint spheroids are consequences of their short nuclear relaxation times [41], the absence of SBHs in these galaxies [42, 43], gas-dynamical processes [44], or some combination of these factors is currently unclear. However the form of a DM crest is essentially independent of $\rho_\star(r)$ (§2) and if the compact nuclei satisfy the other two conditions identified above (presence of a SBH and a significant amount of DM; see discussion below) they would be expected to contain DM crests as well.

If a nucleus is much older than $T_r(r_h)$, a DM crest will form then decay in amplitude as the DM particles attempt to reach equipartition with the much heavier stars (Fig. 1; [24]). Fig. 2 suggests that the crest density drops by a factor 10 from its peak value – corresponding to two orders of magnitude in the annihilation signal – in a time $\sim 8 - 9 T_r(r_h)$. The trends in Fig. 4 are too poorly defined at low values of $L/L_\odot$ to allow us to state clearly for which galaxies this would occur, but a straightforward extrapolation of Eq. (8) suggests that $T_r(r_h)$ falls below $\sim 10^9$ yr at $L \approx 10^{8.7} L_\odot$. If this inference is correct, it follows that crests would be present, with reasonable amplitudes, only for a fairly narrow range of spheroid properties: i.e. spheroids older than $\sim$one relaxation time but younger than many relaxation times. Taking into account the scatter in Fig. 4, the corresponding range in spheroid luminosities might be approximately $3 \times 10^8 L_\odot \lesssim L \lesssim 3 \times 10^9 L_\odot$.

If low-luminosity spheroids do *not* contain massive BHs, nuclear relaxation times might generically be as short as those observed in NGC 205 and M33, i.e. $10^7 - 10^8$ yr. In this case, the stars would undergo core collapse in $\lesssim 10^{10}$ yr producing a $r^{-2.25}$ density profile, and the DM density would be expected to evolve only slightly [45].

At the other extreme of luminosity, galaxies with $L \gtrsim 10^{10} L_\odot$ are always observed to have low-density cores with radii $\sim r_h$ [46, 47, 48], and high central velocity dispersions, implying long nuclear relaxation times (Fig. 4). In principle, these galaxies could still harbor *collisionless* DM spikes around their SBHs [12], but this seems unlikely: the nuclear structure of these galaxies is consistent with no dynamical evolution having occurred since the most recent merger "carved out" the luminous core

[24], and the same merger event that created the stellar core would have destroyed a density spike in the DM [16]. Below we discuss the possibility that *low*-luminosity spheroids might partially retain their steep, collisionless spikes; these galaxies are unlikely to have experienced significant mergers and scattering off of stars need not completely convert such a spike into a weaker, Bahcall-Wolf crest in a Hubble time [24].

B. Black holes

The presence of a massive BH is another necessary condition for the formation of a DM crest. Robust detection of SBHs is possible only in galaxies near enough that the stellar or gas kinematics can be resolved on scales $\ll r_h$. Reliable, dynamical SBH masses have been determined in a handful of such galaxies [10], and the large-scale properties (mass, luminosity, velocity dispersion) of their host spheroids are found to obey tight scaling relations with $M_\bullet$ [49, 50, 51], e.g.

$$M_{\bullet,8} = (1.66 \pm 0.24)\sigma_{200}^{4.86\pm0.43} \tag{9}$$

[10], where $M_{\bullet,8} = M_\bullet/10^8 M_\odot$ and σ_{200} is the 1D stellar velocity dispersion in units of 200 km s^{-1}. The existence of these tight relations suggests that SBHs are ubiquitous in bright spheroids, but the faintest galaxy for which $M_\bullet$ has been robustly determined is M32 ($L \approx 4 \times 10^8 L_\odot$; in fact this galaxy is believed to be the remnant core of a once much brighter galaxy) and it is dangerous to assume that relations like (9) apply to fainter systems, including the spheroids with $L \lesssim 10^9 L_\odot$ that are most relevant to formation of crests (Fig. 4).

Evidence for massive BHs in spheroids fainter than $\sim 10^9 L_\odot$ – dwarf elliptical galaxies and the bulges of late-type spiral galaxies – comes almost entirely from the subset of nuclei that are "active," i.e. that emit a significant fraction of their energy non-thermally [52]. $M_\bullet$ in these galaxies is determined indirectly by applying empirical relations established in more luminous active galaxies, e.g. between the size of the so-called broad emission line region and the nuclear continuum luminosity [53]. The presence of BHs with masses as low as $\sim 10^5 M_\odot$ has been inferred [54]; with one exception (POX 52, a dwarf elliptical galaxy [55]), all of the host spheroids are spiral-galaxy bulges. The BH masses in these galaxies appear to be consistent with relations like (9) [56].

Whether BHs with $M_\bullet \lesssim 10^6 M_\odot$, are present in all low-luminosity spheroids is still unclear. In the Local Group, neither the dwarf elliptical NGC 205 ($L \approx 10^{8.4} L_\odot$) or M33 (an apparently spheroid-less spiral galaxy) appear to have central BHs although the upper limits on $M_\bullet$ in these galaxies (based on stellar kinematics) are only marginally inconsistent with the scaling relations established in brighter galaxies [40, 57]. A significant fraction ($\sim 40\%$) of nearby galaxies show evidence of low-level nuclear activity but the activity need not be driven by BH accretion in every case [52]. Even if

small BHs were present at one time in all low-luminosity spheroids, a number of processes are capable of ejecting them from such environments [58].

Some nuclei might contain binary or multiple BHs, if the BHs that were deposited there during a galaxy merger failed to coalesce. In the presence of a binary SBH, growth of a collisional cusp would be inhibited as the binary continued to eject stars and DM particles from the nucleus via the gravitational slingshot [59]. Time scales for binary SBH coalescence due to gravitational wave emission are longer than 10^{10} yr unless the binary separation a drops below

$$a_{GW} \approx 2 \times 10^{-3}\text{pc}\frac{q}{(1+q)^2}M_{12,6}^3 \tag{10}$$

where $q = M_2/M_1 \le 1$ is the binary mass ratio and $M_{12,6} = (M_1 + M_2)/10^6 M_\odot$ [60]. This separation is $1-2$ orders of magnitude less than the separation a_h at which the two BHs become gravitationally bound, and it is possible for the binary to stall at $a \approx a_h \gg a_{GW}$ (the "final parsec problem"). Stalling is least likely in nuclei with short relaxation times, since stars will scatter into the binary's sphere of influence where they can extract angular momentum from the binary [61, 62]. A number of other mechanisms have been identified that can accelerate the evolution of binary SBHs, even in collisionless nuclei [63, 64]. Constraints on the binarity of the MW SBH are fairly tight [60], and only one clear detection of a binary SBH has so far been made [65], suggesting that they may be rare.

C. Dark matter

Detectability of DM crests depends critically on the DM density at r_h, roughly the outer boundary of the region in which the mass distribution is modified by the (single or binary) SBH. Traditionally there have been two approaches to estimating ρ_χ at the centers of galaxies; unfortunately they lead to rather different conclusions about $\rho_\chi(r_h)$.

N-body simulations of gravitational clustering follow the growth of DM halos as they evolve via mergers in an expanding, cold-dark-matter (ΛCDM) universe. Halo density profiles in these simulations are well determined on scales $10^{-2} \lesssim r/r_{vir} \lesssim 10^0$, where the virial radius r_{vir} is of order 10^2 kpc for a galaxy like the Milky Way; hence inferences about ρ_χ on scales of $r_h \approx 10^{-3}$ kpc require a radical extrapolation from the N-body results. A standard parametrization of ρ_χ in these simulated halos is

$$\rho_\chi(r) = \rho_0 \xi^{-1} (1 + \xi)^{-2} \tag{11}$$

[66], the "NFW profile," where $\xi = r/r_s$ and r_s is a scale length of order r_{vir}. In the Milky Way, $r_{vir} \gg R_\odot$ (the radius of the Solar circle) hence Eq. (11) is essentially a power law at $r < R_\odot$ and the implied DM density at r_h

is

$$\rho_\chi(r_h) \approx 30 M_\odot \text{pc}^{-3} \left(\frac{\rho_\odot}{10^{-2} M_\odot \text{pc}^{-3}} \right) \left(\frac{R_\odot}{8 \text{ kpc}} \right) \left(\frac{r_h}{3 \text{ pc}} \right)^{-1} \quad (12)$$

where $\rho_\odot \equiv \rho_\chi(R_\odot)$ and $\rho_\odot \approx 8 \times 10^{-3} M_\odot \text{pc}^{-3}$ (from the Galactic rotation curve). Moore et al. [67] argue for a steeper inner slope, $\rho_\chi \sim r^{-1.5}$, implying $\rho_\chi(r_h) \approx 10^3 M_\odot \text{pc}^{-3}$. Still higher DM densities could exist if the baryons (stars, gas) lose energy radiatively and contract, deepening the potential well and pulling in the DM (e.g. [68]). Based on halo scaling relations [69], DM densities at r_h would be higher in spheroids fainter than that of the Milky Way.

Rotation-curve studies of dark-matter-dominated galaxies are generally interpreted as implying much lower, central DM densities [70, 71, 72, 73, 74]. While there are caveats to this interpretation – systematic biases in long-slit observations [75], non-circular motions [76], gas pressure [77], etc. – these effects do not seem capable of fully explaining the discrepancies between rotation curve data and expressions like (11) [73, 78]. A model for $\rho_\chi(r)$ that is often fit to rotation curve data is [70],

$$\rho_\chi(r) = \rho_c \left(1 + \xi \right)^{-1} \left(1 + \xi^2 \right)^{-1}, \quad (13)$$

the "Burkert profile,", where $\xi \equiv r/r_c$ and r_c is the core radius. Inferred core radii are $\sim 10^3$ pc and inferred central densities typically lie in the range $\rho_c \approx (1-5) \times 10^{-2} M_\odot \text{pc}^{-3}$.

Several resolutions have been suggested for this apparent conflict between theory and observation [79]. Since the N-body halos are not resolved on the scales ($\sim 10^2$ pc) where rotation curves are typically measured, the mismatch may simply be due to a poor choice of empirical model used to parametrize $\rho_\chi(r)$. For instance, the alternative parametrization

$$\rho_\chi(r) = \rho' \xi^{-p} \exp \left(-b \xi^{1/n} \right), \quad (14)$$

the "Prugniel-Simien" law [80], is both a better fit to the N-body data than Eq. (11) and is also in reasonable accord with rotation curve data [69, 81, 82, 83]. Here $\xi \equiv r/R_e$ and R_e is the radius containing $1/2$ of the projected halo mass (the relation between R_e and the virial radius is discussed in [84]). The profile shape in Eq. (14) is determined by the curvature parameter n; for the N-body halos, n is found to be a weak function of halo mass, but exhibits a substantial scatter at all halo masses,

$$2 \lesssim n \lesssim 6 \quad (15)$$

(e.g. [84], Fig. 1a). The constants b and p in Eq. (14) are determined uniquely by n [83]; for the range in n cited above, $0.7 \lesssim p \lesssim 0.9$, i.e. the density increases more slowly toward the center than the NFW [66] ($\propto r^{-1}$) profile.

D. Summary of Galaxy Properties Relevant to the Formation of Crests

Relaxation times are short enough for the formation of DM crests in stellar spheroids with $L \approx 10^{9.5} L_\odot$ or fainter. However the nuclear structure of faint galaxies is typically unresolved and relaxation times in spheroids with $L \lesssim 10^9 L_\odot$ are uncertain. SBHs appear to be ubiquitous in stellar spheroids brighter than $\sim 10^9 L_\odot$, with masses that are well predicted by the properties of the stellar spheroid via empirical scaling relations. A handful of massive ($\sim 10^5 M_\odot$) BHs have been detected in fainter galaxies via their non-thermal spectral features, but it is not clear what fraction of low-luminosity spheroids contain BHs. Dark matter densities at $r \approx r_h$ in spheroids with $L \approx 10^9 L_\odot$ may be as high as $10^2 - 10^3 M_\odot \text{pc}^2$, if standard parametrizations of ΛCDM halo models are correct; or as low as $\sim 10^{-2} - 10^{-1} M_\odot \text{pc}^{-3}$ if rotation curve studies are to be believed.

V. OBSERVABILITY OF THE CRESTS

In this section, we consider the implications of collisionally-generated DM crests for the rate of particle self-annihilations and for the detectability of the resultant gamma rays. We consider separately the case of the Milky Way and external galaxies. Since the $\rho_\chi \sim r^{-3/2}$ crests considered here are relatively weak (e.g. compared with the steeper spikes that form via adiabatic growth of a SBH, $\rho_\chi \sim r^{-\gamma}$, $2 \lesssim \gamma \lesssim 3$ [12]), we focus on the question of whether the DM distribution inferred above at $r \lesssim r_h$ implies a substantial *increase* in the predicted annihilation signal compared with the signal from a galaxy that lacks such a crest.

The annihilation rate from neutralinos near the center of a spherically-symmetric DM halo is proportional to $\int \rho_\chi^2(r) r^2 dr$. In the presence of a $\rho_\chi \sim r^{-3/2}$ crest, the integral diverges as $\log(r_0^{-1})$ where r_0 is the inner radius of the crest. Roughly, r_0 is the maximum of (r_S, r_a) where $r_S = 2GM_\bullet/c^2$ is the Schwarzschild radius of the SBH and r_a is the radius where the self-annihilation time equals $\sim T_r$. For all reasonable values of m_χ and σv, the annihilation cross section, $r_a \ll r_S$ hence we assume $r_0 \approx r_S$ in what follows.

Evaluating this integral in the case of the N-body density profile of Fig. 3 at $t = T_r(r_h)$, we find

$$\int_{r_0}^{\infty} \rho_\chi^2(r) r^2 dr = \rho_h^2 r_h^3 \left[C_1 \ln \left(\frac{r_h}{r_0} \right) + C_2 \right] \quad (16)$$

with $C_1 \approx 4.22 \times 10^{-2}$, $C_2 \approx 2.94$ and $\rho_h \equiv \rho_\chi(r_h)$. (We assumed $\rho_\chi(r) = \rho_1 (r/r_1)^{-3/2}$ at $r \leq r_1 = 0.01 r_h$ where the N-body density is poorly defined, as justified above.) Roughly 90% of the integral comes from matter at $r \leq r_h$.

While the DM density is affected by the SBH at all $r \lesssim r_h$, the $\rho_\chi \sim r^{-3/2}$ crests only extend out to $r \lesssim 0.1 r_h$.

We find that $\sim 20\%$ of the integral (16) comes from the crest proper, i.e. from $r \lesssim 0.1 r_h$.

Setting $\ln(r_h/r_0) \approx \ln(c^2/v_{rms}^2) \approx 15$, the integral in Eq. (16) is $\sim 3.6 \rho_h^2 r_h^3$. For comparison, the value corresponding to a constant density within r_h is $\sim 0.33 \rho_h^2 r_h^3$.

Henceforth we assume that Fig. 3 correctly represents the DM distribution at $r \lesssim r_h$ in nuclei that are $\sim T_r(r_h)$ old, i.e. that

$$\int_{r_0}^{r_h} \rho_\chi^2(r) r^2 dr \approx 3 \rho_h^2 r_h^3. \qquad (17)$$

The observable annihilation signal will typically include a contribution from $r \leq r_h$, as well as a contribution from DM beyond r_h that lies within the detector's window. We will consider several possible forms for the large-radius dependence of ρ_χ on r.

At times later than $\sim T_r(r_h)$, the amplitude of the crest drops due to continued heating from the stars (e.g. Fig. 2). We discuss the consequences of this effect for the observability of crests in more detail below.

A. Milky Way

The photon flux from neutralino annihilations in the Galactic halo, observed by a detector with angular acceptance $\Delta\Omega$, is

$$\Phi(E) = \frac{1}{2} \frac{\sigma v}{m_\chi^2} \frac{dN}{dE} I(\Delta\Omega), \qquad (18a)$$

$$I(\Delta\Omega) = \frac{1}{4\pi} \int_{\Delta\Omega} d\Omega' \int \rho_\chi^2(l) dl. \qquad (18b)$$

Here σv is the annihilation cross section times relative velocity (in the nonrelativistic limit), dN/dE is the gamma ray spectrum per annihilation, and l is the line-of-sight distance. In the case of telescope centered on the Milky Way SBH, the integral can be written

$$\begin{aligned} I(\Psi) \approx \frac{1}{R_\odot^2} \Bigg[&\int_{r_0}^{r_h} \rho_\chi^2(r) r^2 dr \\ &+ \int_{r_h}^{\Psi R_\odot} \rho_\chi^2(r) r^2 dr \\ &+ \int_{\Psi R_\odot}^{R_\odot} \rho_\chi^2 \left(r^2 - r\sqrt{r^2 - \Psi^2 R_\odot^2} \right) \Bigg] \end{aligned} \qquad (19)$$

where $\Psi^2 \equiv \Delta\Omega/\pi$; the inequality reflects the omission of the contribution from DM outside the Solar circle, and we have also implicitly assumed $\Psi R_\odot > r_h$, valid for all current and planned detectors. (Atmospheric Cerenkov telescopes like HESS, and the proposed satellite observatory GLAST, have $\Delta\Omega \approx 5 \times 10^{-5}$ sr.) We equate the first term on the RHS of Eq. (19) with Eq. (17). To evaluate the additional terms we require $\rho_\chi(r)$ at $r > r_h$. A simple model is a power-law,

$$\rho_\chi(r) = \rho_\chi(r_h) (r/r_h)^{-\gamma}, \quad r > r_h. \qquad (20)$$
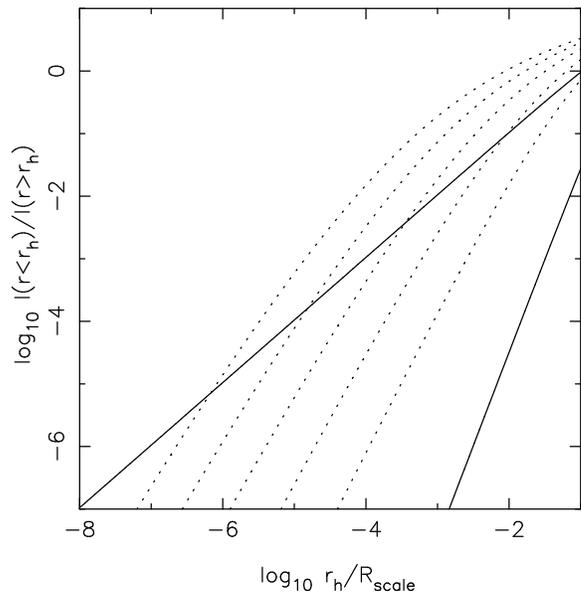

FIG. 5: Contribution to the self-annihilation signal from DM at $r \leq r_h$, i.e. within the SBH's influence radius. The DM distribution at $r \leq r_h$ is assumed to be the same as in Fig. 3 at $t = T_r(r_h)$. Three different models for the DM density at $r > r_h$ have been evaluated: *Lower solid line:* Burkert profile; *Upper solid line:* NFW profile; *Dotted lines:* Prugniel-Simien profile, with $n = (2, 3, 4, 5, 6)$, increasing upwards. R_{scale} is the appropriate scale length for each model, i.e. r_c (Burkert), r_s (NFW), R_e (Prugniel-Simien).

For $\gamma = 1$ this is a reasonable approximation to both an NFW profile, Eq. (11), and a Prugniel-Simien profile, Eq. (14), at $r < R_\odot$. Setting $\gamma = 1$ gives

$$I(\Psi) \approx \rho_\chi^2(r_h) r_h^3 R_\odot^{-2} \left(3 + \frac{\pi}{2} \frac{\Psi R_\odot}{r_h} - 1 \right) \qquad (21)$$

where the first term is the contribution from $r \leq r_h$ (Fig. 3). For $\Delta\Omega = 5 \times 10^{-5}$ ($\Psi \approx 4 \times 10^{-3}$ sr), roughly 20% of I is due to matter at $r \leq r_h$ and roughly 4% from the crest proper. This result suggests that the detectability of DM self-annihilations at the Galactic center is not likely to be significantly affected by the presence of a crest. We note that in Ref. [25], the contribution of a DM crest at the Galactic center to the self-annihilation signal was found to be much greater. The discrepancy arises from the fact that these authors ignored the third (dominant) term on the right hand side of Eq. (19), and they assumed that the crest extended as $\rho_\chi \propto r^{-3/2}$ all the way to r_h, rather than to only a fraction of r_h.

The relative contribution from the crest could be increased by assuming a steeper DM density falloff, e.g. in a halo where the DM had been pulled in by contraction of the baryons, or a smaller angular acceptance $\Delta\Omega$ of the detector. As discussed above, observations favor a *lower* DM density implying even less of a contribution from the crest.

B. External Galaxies

In the case of a detector centered on the SBH of an external galaxy, the geometrical term in the expression for the flux becomes

$$I = \frac{1}{D^2} \int \rho_\chi^2(r) r^2 dr \qquad (22)$$

where D is the distance to the galaxy and the integral includes as much of the galaxy as is imaged by the telescope; thus

$$I(\Psi) = \frac{1}{D^2} \left[\int_{r_0}^{r_h} \rho_\chi^2(r) r^2 dr + \int_{r_h}^{\Psi D} \rho_\chi^2(r) r^2 dr \right]. \quad (23)$$

We again equate the first term in brackets with Eq. (17). For the low-luminosity galaxies that are likely to harbor a DM crest (Sect. IVA), the gamma-ray telescope would image essentially the entire halo and so we set the upper limit of the second integral to infinity in what follows.

Following the discussion in Sect. IIIC, we considered three possible forms for the DM density beyond $r = r_h$: the NFW profile (Eq. 11), the Burkert profile (Eq. 13) and the Prugniel-Simien profile (Eq. 14).

Fig. 5 shows the relative contribution of the DM at $r \leq r_h$ to the annihilation signal for the three assumed DM profiles. In the case of the Prugniel-Simien profile, the curvature parameter n has been varied over the range $2 \leq n \leq 6$ that approximately characterizes the N-body haloes [83]. The contribution of the crest is insignificant in the case of the Burkert profile and only significant in the case of the NFW profile if r_h/r_s is unphysically large. For the Prugniel-Simien profile however, the crest adds significantly to the total signal for large n and $r_h/R_e \gtrsim 10^{-4}$.

Whether such large values of r_h/R_e are physically reasonable depends on the poorly-understood relations between SBH mass, galaxy mass and DM halo properties at the low-mass end of these distributions. The scale radii R_e of N-body DM halos obey

$$\frac{R_e}{100 \text{ kpc}} \approx 1.1 \left(\frac{M_{DM}}{10^{12} M_\odot} \right)^{1/2} \qquad (24)$$

[69]. Thus

$$\frac{r_h}{R_e} \approx \frac{GM_\bullet}{\sigma_\star^2 R_e}$$

$$\approx 4 \times 10^{-6} \left(\frac{M_\bullet}{10^6 M_\odot} \right) \left(\frac{\sigma_\star}{100 \text{ km s}^{-1}} \right)^{-2} \left(\frac{M_{DM}}{10^{12} M_\odot} \right)^{-1/2} \quad (25)$$

Adopting the empirical relation between $M_\bullet$ and $\sigma_\star$ [10]

$$\frac{M_\bullet}{10^6 M_\odot} \approx 5.7 \left(\frac{\sigma_\star}{100 \text{ km s}^{-1}} \right)^\alpha, \quad \alpha \approx 4.86 \qquad (26)$$

(which has only been established for $\sigma_\star \gtrsim 100$ km s^{-1}) this becomes

$$\frac{r_h}{R_e} \approx 8 \times 10^{-6} \left(\frac{M_\bullet}{10^6 M_\odot} \right)^{0.59} \left(\frac{M_{DM}}{10^{12} M_\odot} \right)^{-1/2}. \quad (27)$$

If $M_\bullet$ scales linearly with halo mass at the low-mass end of the distribution, this relation implies that r_h/R_e is essentially independent of $M_\bullet$ and M_{DM}, hence roughly equal to its value in the Milky Way, $r_h/R_e \approx 1 \times 10^{-5}$.

On the other hand, the empirical relation between rotation curve peak velocity and stellar velocity dispersion suggests a nonlinear relation between $M_\bullet$ and M_{DM}, of the approximate form [85]

$$\frac{M_\bullet}{10^6 M_\odot} \approx K \left(\frac{M_{DM}}{10^{12} M_\odot} \right)^\beta \qquad (28)$$

with $1.5 \lesssim \beta \lesssim 2$ and $0.1 \lesssim K \lesssim 1$. Thus

$$\frac{r_h}{R_e} \propto M_\bullet^{0.59 - 1/2\beta} \propto M_{DM}^{0.59\beta - 1/2} \qquad (29)$$

and r_h/R_e would scale approximately as $M_\bullet^{0.3} \propto M_{DM}^{0.6}$.

These scaling relations should be considered highly uncertain for the reasons discussed in Sect. IV. A third possibility, not inconsistent with the limited observational constraints on SBH and halo masses, is that SBH mass is essentially independent of halo mass at the low-mass end of the distributions. This assumption would imply increasing values of r_h/R_e in dwarf galaxies, hence larger contributions from the crests to the annihilation signal (Fig. 5).

C. Dependence on initial conditions and galaxy age

The estimates made above of DM crest observability were based on the N-body density profile, Fig. 3, at $t = T_r(r_h)$. While this density profile is "universal" at $r \lesssim 0.1r_h$ in the sense that $\rho_\chi \sim r^{-3/2}$ is a steady-state solution to the Fokker-Planck equation in a point-mass potential, the amplitude of the crest decays after its formation due to continued heating by the stars (Fig. 2; [17, 24]). Furthermore the distribution of DM within the SBH's influence radius could be different if the initial conditions were very different from those assumed here.

Initial conditions: Until now we have made the conservative assumption that the DM density profile was initially very flat near the center. These are appropriate initial conditions if the galaxy hosting the DM experienced a merger following formation of SBHs, since a binary SBH is efficient at ejecting matter from the center of a galaxy and creating a low-density core [16]. However the mean time between mergers is a strong function of galaxy luminosity/mass, and an isolated, low-mass stellar spheroid might not have experienced a significant merger in the last 10^{10} yr. (We note that this statement does not apply to the bulges of massive spiral galaxies, like

that of the Milky Way, since the merger probability is determined by the overall mass/radius of the galaxy, and these are much larger than the mass/radius of the bulge in the case of a spiral galaxy.) For instance, intermediate-mass black holes (IMBHs) might have formed via direct collapse of primordial gas in low-mass halos [86]. In this scenario, the distribution of DM around the IMBH could have the steep dependence with radius predicted by so-called "adiabatic growth" models, $\rho_\chi \sim r^{-\gamma}, 2 \lesssim \gamma \lesssim 3$ [87, 88]. Such steep spikes would be "softened" by self-annihilations at small radii and by heating from the stars, but Fokker-Planck integrations show that the density profile after one relaxation time can remain considerably steeper than that of the collisional, $\rho_\chi \sim r^{-3/2}$ crests discussed here [17, 24]. The same considerations would apply to a spike in a more massive halo that did not happen to experience a major merger since the epoch of SBH formation.

Age: On time scales long compared with $T_r(r_h)$, continued collisional evolution of a nucleus can result in different stellar and/or DM density profiles at $r \lesssim r_h$. Heating of DM by stars causes the normalization of the DM density to drop, while roughly maintaining the $\rho_\chi \sim r^{-3/2}$ dependence at $r \ll r_h$ (e.g. Fig. 1, 2). Capture or tidal disruption of stars by the SBH is effectively a heat source, causing a nucleus to expand [89]; the time scale is of order $\sim T_r(r_h)$ and depends on the sizes and masses of stars. If there is a range of stellar masses, the more massive stars will accumulate near the center, causing the stellar mass density profile to become more centrally peaked [11]. While the "steady-state" functional form for $\rho_\chi(r)$, Eq. (7), is formally independent of $\rho_\star(r)$, the rate at which the stars transfer energy to the DM depends on the stellar density. As discussed above (Sect. IV A), it is not clear that any nucleus harboring a SBH is much older than one relaxation time.

VI. SUMMARY

By considering the joint evolution of the stellar and dark-matter (DM) densities at the center of a galaxy con-taining a supermassive black hole (SBH), we have shown that the existence of a "crest" (collisionally regenerated dark-matter structure) can be robustly predicted in any nucleus old enough to have generated a Bahcall-Wolf cusp in the stars. This time scale is roughly 10 Gyr in the case of the Milky Way, and probably shorter for fainter galaxies that contain massive BHs. Crest generation occurs even in the (probably generic) case of a nucleus that previously experienced the scouring effect of a binary SBH. Standard galaxy scaling relations suggest that crests do not dramatically change the prospects for indirect detection of DM. However this conclusion could be modified if the DM density falls steeply beyond the SBH's gravitational influence radius, or if SBH masses scale weakly with DM halo masses. In any case, crest formation implies a significant increase in the density of DM around the central SBH, and the presence of crests should be taken into account when studying the constraints on the annihilation rate from stellar orbits [90], or the evolution of stars in the innermost regions of galactic nuclei [91, 92].

VII. ACKNOWLEDGEMENTS

[1] G. Bertone, D. Hooper, and J. Silk, Physics Reports **405**, 279 (2004).

[2] L. Bergstrom, Rept. Prog. Phys. **63**, 793 (2000), hep-ph/0002126.

[3] G. Bertone and D. Merritt, Modern Physics Letters A **20**, 1021 (2005).

[4] J. Carr, G. Lamanna, and J. Lavalle, Reports of Progress in Physics **69**, 2475 (2006).

[5] F. W. Stecker, Physics Letters B **201**, 529 (1988).

[6] L. Bergström, P. Ullio, and J. H. Buckley, Astroparticle Physics **9**, 137 (1998).

[7] G. Bertone, G. Sigl, and J. Silk, Monthly Notices of the Royal Astronomical Society **326**, 799 (2001).

[8] N. Fornengo, L. Pieri, and S. Scopel, Phys. Rev. D **70**, 103529 (2004).

[9] D. Hooper, I. de la Calle Perez, J. Silk, F. Ferrer, and S. Sarkar, Journal of Cosmology and Astro-Particle Physics **9**, 2 (2004).

[10] L. Ferrarese and H. Ford, Space Science Reviews **116**, 523 (2005).

[11] D. Merritt, Reports on Progress in Physics **69**, 2513 (2006).

[12] P. Gondolo and J. Silk, Physical Review Letters **83**, 1719 (1999).

[13] G. Bertone, G. Sigl, and J. Silk, Mon. Not. Roy. Astron. Soc. **337**, 98 (2002), astro-ph/0203488.

[14] R. Aloisio, P. Blasi, and A. V. Olinto, Journal of Cosmology and Astro-Particle Physics **5**, 7 (2004).

[15] P. Ullio, H. Zhao, and M. Kamionkowski, Phys. Rev. D **64**, 043504 (2001).

[16] D. Merritt, M. Milosavljević, L. Verde, and R. Jimenez, Physical Review Letters **88**, 191301 (2002).

[17] G. Bertone and D. Merritt, Phys. Rev. D **72**, 103502 (2005).

[18] D. Merritt, The Astrophysical Journal **648**, 000 (2005).

[19] T. R. Lauer, S. M. Faber, E. A. Ajhar, C. J. Grillmair, and P. A. Scowen, Astronomical Journal **116**, 2263 (1998).

[20] T. Alexander, Astrophys. J. **527**, 835 (1999).

[21] J. N. Bahcall and R. A. Wolf, Astrophys. J. **209**, 214 (1976).

[22] D. Merritt and A. Szell, The Astrophysical Journal **648**, 000 (2005).

[23] A. S. Ilyin, K. P. Zybin, and A. V. Gurevich, Journal of Experimental and Theoretical Physics **98**, 1 (2004).

[24] D. Merritt, Physical Review Letters **92**, 201304 (2004).

[25] O. Y. Gnedin and J. R. Primack, Physical Review Letters **93**, 061302 (2004).

[26] M. Hénon, Annales d'Astrophysique **24**, 369 (1961).

[27] L. Spitzer, *Dynamical evolution of globular clusters* (Princeton, NJ, Princeton University Press, 191 p., 1987).

[28] D. Merritt, Astrophys. J. **264**, 24 (1983).

[29] J. N. Bahcall and R. A. Wolf, Astrophys. J. **216**, 883 (1977).

[30] W. Dehnen, Monthly Notices of the Royal Astronomical Society **265**, 250 (1993).

[31] S. Harfst, A. Gualandris, D. Merritt, R. Spurzem, S. Portegies Zwart, and P. Berczik, ArXiv Astrophysics e-prints (2006).

[32] J. Makino and M. Taiji, *Scientific simulations with special-purpose computers : The GRAPE systems* (Toronto, John Wiley and Sons, 1998).

[33] L. Ferrarese, P. Côté, A. Jordán, E. W. Peng, J. P. Blakeslee, S. Piatek, S. Mei, D. Merritt, M. Milosavljević, J. L. Tonry, et al., Astrophys. J. Supplement **164**, 334 (2006).

[34] A. M. Ghez, S. Salim, S. D. Hornstein, A. Tanner, J. R. Lu, M. Morris, E. E. Becklin, and G. Duchêne, Astrophys. J. **620**, 744 (2005).

[35] M. Preto, D. Merritt, and R. Spurzem, Astrophys. J. Letters **613**, L109 (2004).

[36] H. Baumgardt, J. Makino, and T. Ebisuzaki, Astrophys. J. **613**, 1133 (2004).

[37] P. Côté, S. Piatek, L. Ferrarese, A. Jordán, D. Merritt, E. W. Peng, M. Haşegan, J. P. Blakeslee, S. Mei, M. J. West, et al., Astrophys. J. Supplement **165**, 57 (2006).

[38] H. Baumgardt, J. Makino, and T. Ebisuzaki, Astrophys. J. **613**, 1143 (2004).

[39] T. Böker, M. Sarzi, D. E. McLaughlin, R. P. van der Marel, H.-W. Rix, L. C. Ho, and J. C. Shields, Astronomical Journal **127**, 105 (2004).

[40] M. Valluri, L. Ferrarese, D. Merritt, and C. L. Joseph, Astrophys. J. **628**, 137 (2005).

[41] L. Hernquist, P. Hut, and J. Kormendy, Nature (London) **354**, 376 (1991).

[42] L. Ferrarese, P. Côté, E. Dalla Bontà, E. W. Peng, D. Merritt, A. Jordán, J. P. Blakeslee, M. Haşegan, S. Mei, S. Piatek, et al., Astrophys. J. Letters **644**, L21 (2006).

[43] E. H. Wehner and W. E. Harris, Astrophys. J. Letters **644**, L17 (2006), astro-ph/0603801.

[44] D. E. McLaughlin, A. R. King, and S. Nayakshin, ArXiv Astrophysics e-prints (2006), astro-ph/0608521.

[45] E. Kim, H. M. Lee, and R. Spurzem, Monthly Notices of the Royal Astronomical Society **351**, 220 (2004).

[46] M. Milosavljević, D. Merritt, A. Rest, and F. C. van den Bosch, Monthly Notices of the Royal Astronomical Society **331**, L51 (2002).

[47] S. Ravindranath, L. C. Ho, and A. V. Filippenko, Astrophys. J. **566**, 801 (2002).

[48] A. W. Graham, Astrophys. J. Letters **613**, L33 (2004).

[49] L. Ferrarese and D. Merritt, Astrophys. J. Letters **539**, L9 (2000).

[50] A. W. Graham, P. Erwin, N. Caon, and I. Trujillo, Astrophys. J. Letters **563**, L11 (2001).

[51] A. Marconi and L. K. Hunt, Astrophys. J. Letters **589**, L21 (2003).

[52] L. C. W. Ho, in *Coevolution of Black Holes and Galaxies*, edited by L. C. Ho (2004), pp. 292–+.

[53] S. Kaspi, P. S. Smith, H. Netzer, D. Maoz, B. T. Jannuzi, and U. Giveon, Astrophys. J. **533**, 631 (2000).

[54] J. E. Greene and L. C. Ho, Astrophys. J. **610**, 722 (2004).

[55] A. J. Barth, L. C. Ho, R. E. Rutledge, and W. L. W. Sargent, Astrophys. J. **607**, 90 (2004).

[56] A. J. Barth, J. E. Greene, and L. C. Ho, Astrophys. J. Letters **619**, L151 (2005).

[57] D. Merritt, L. Ferrarese, and C. L. Joseph, Science **293**, 1116 (2001).

[58] D. Merritt, M. Milosavljević, M. Favata, S. A. Hughes, and D. E. Holz, Astrophys. J. Letters **607**, L9 (2004).

[59] S. Mikkola and M. J. Valtonen, Monthly Notices of the Royal Astronomical Society **259**, 115 (1992).

[60] D. Merritt and M. Milosavljević, Living Reviews in Relativity **8**, 8 (2005).

[61] Q. Yu, Monthly Notices of the Royal Astronomical Society **331**, 935 (2002).

[62] M. Milosavljević and D. Merritt, Astrophys. J. **596**, 860 (2003).

[63] P. Berczik, D. Merritt, R. Spurzem, and H.-P. Bischof, Astrophys. J. Letters **642**, L21 (2006).

[64] A. I. Macfadyen and M. Milosavljevic, ArXiv Astrophysics e-prints (2006).

[65] C. Rodriguez, G. B. Taylor, R. T. Zavala, A. B. Peck, L. K. Pollack, and R. W. Romani, Astrophys. J. **646**, 49 (2006).

[66] J. F. Navarro, C. S. Frenk, and S. D. M. White, Astrophys. J. **462**, 563 (1996).

[67] B. Moore, F. Governato, T. Quinn, J. Stadel, and G. Lake, Astrophys. J. Letters **499**, L5+ (1998).

[68] F. Prada, A. Klypin, J. Flix, M. Martínez, and E. Simonneau, Physical Review Letters **93**, 241301 (2004).

[69] A. W. Graham, D. Merritt, B. Moore, J. Diemand, and B. Terzic, ArXiv Astrophysics e-prints (2006), astro-ph/0608614.

[70] A. Burkert, Astrophys. J. Letters **447**, L25+ (1995).

[71] P. Salucci and A. Burkert, Astrophys. J. Letters **537**, L9 (2000).

[72] W. J. G. de Blok and A. Bosma, Astronomy and Astrophysics **385**, 816 (2002).

[73] G. Gentile, A. Burkert, P. Salucci, U. Klein, and F. Walter, Astrophys. J. Letters **634**, L145 (2005).

[74] W. J. G. de Blok, Astrophys. J. **634**, 227 (2005).

[75] K. Spekkens, R. Giovanelli, and M. P. Haynes, Astronomical Journal **129**, 2119 (2005).

[76] J. D. Simon, A. D. Bolatto, A. Leroy, L. Blitz, and E. L. Gates, Astrophys. J. **621**, 757 (2005).

[77] O. Valenzuela, G. Rhee, A. Klypin, F. Governato, G. Stinson, T. Quinn, and J. Wadsley, ArXiv Astrophysics e-prints (2005), astro-ph/0509644.

[78] W. J. G. de Blok, in *IAU Symposium*, edited by S. Ryder, D. Pisano, M. Walker, and K. Freeman (2004), pp. 69–+.

[79] A. Tasitsiomi, International Journal of Modern Physics D **12**, 1157 (2003).

[80] P. Prugniel and F. Simien, Astron. Astrophys. **321**, 111 (1997).

[81] J. F. Navarro, E. Hayashi, C. Power, A. R. Jenkins, C. S. Frenk, S. D. M. White, V. Springel, J. Stadel, and T. R. Quinn, Mon. Not. R. Astron. Soc. **349**, 1039 (2004).

[82] D. Merritt, J. F. Navarro, A. Ludlow, and A. Jenkins, Astrophys. J. Letters **624**, L85 (2005).

[83] D. Merritt, A. W. Graham, B. Moore, J. Diemand, and B. Terzic, ArXiv Astrophysics e-prints (2005), astro-ph/0509417.

[84] A. W. Graham, D. Merritt, B. Moore, J. Diemand, and B. Terzic, ArXiv Astrophysics e-prints (2006), astro-ph/0608613.

[85] L. Ferrarese, Astrophys. J. **578**, 90 (2002), astro-ph/0203469.

[86] S. M. Koushiappas, J. S. Bullock, and A. Dekel, MNRAS **354**, 292 (2004), astro-ph/0311487.

[87] G. Bertone, A. R. Zentner, and J. Silk, Phys. Rev. **D72**, 103517 (2005), astro-ph/0509565.

[88] G. Bertone, Phys. Rev. **D73**, 103519 (2006), astro-ph/0603148.

[89] S. L. Shapiro, Astrophys. J. **217**, 281 (1977).

[90] J. Hall and P. Gondolo, Phys. Rev. **D74**, 063511 (2006), astro-ph/0602400.

[91] P. Salati and J. Silk, Astrophys. J. **338**, 24 (1989).

[92] I. V. Moskalenko and L. Wai (2006), astro-ph/0608535.